Multitemporal Wetland Monitoring in Sub-Saharan West-Africa Using Medium Resolution Optical Satellite Data

Linda Moser, Stefan Voigt, Elisabeth Schoepfer, and Stephanie Palmer

***Abstract*—Surface water is a critical resource in semiarid West-African regions that are frequently exposed to droughts. Natural and artificial wetlands are of high importance for different livelihoods, particularly during the dry season, from October/November until May. However, wetlands largely go unmonitored. In this work, remote sensing is used to monitor wetlands in semiarid Burkina Faso over large areal extents along a gradient of different rainfall and land use characteristics. Time series of data from the Moderate Resolution Imaging Spectrometer (MODIS) from 2000 to 2012 is used for near-infrared (NIR)-based water monitoring using a latitudinal threshold gradient approach. The occurrence of 21 new water bodies with a size larger than $0.5\ \mathrm{km}^2$ over the 13-year analysis period results from a postclassification change detection. Yearly cumulative spatiotemporal analysis shows lower water extents in the drought seasons of 2000–2001, 2004–2005, and 2011–2012. Multiple wetlands indicate a positive trend toward a larger yearly maximum area, but a negative trend toward shorter flooding duration. Such a negative trend is observed particularly for natural wetlands. The temporal behavior of five selected case studies demonstrates that monthly negative anomalies of water-covered areas coincide with the occurrence of drought seasons. The successful application of remote sensing time series as a tool to monitor wetlands in semiarid regions is presented, and the potential of novel early warning indicators of drought from remote sensing is demonstrated.**

***Index Terms*—Burkina Faso, drought indicators, Moderate Resolution Imaging Spectrometer (MODIS), monitoring, Sahel, surface water, time series, wetlands.**

I. Introduction

THE WEST-AFRICAN Sahel belt was subjected to devastating droughts between the years 1910–1916, 1941–1945, and particularly devastating droughts in the mid-1970s and mid-1980s leading to food crises. These drought periods are coupled with negative precipitation anomalies with respect to the last 110 years. In comparison to pre-1970 precipitation conditions, the drought can be considered to be ongoing at present, although an increasing precipitation trend is detectable over the last 15–20 years [1], [2]. Most recently, in 2012, the West-African Sahel region (particularly Mali, Mauritania, Niger, and Burkina Faso) suffered from a severe drought and hunger crisis [3]–[5]. Burkina Faso is a water scarce country, and according to the commonly used Falkenmark water stress index [6], it has only $820.5\ \mathrm{m}^3\ \mathrm{inhabitant}^{-1}\ \mathrm{year}^{-1}$ of total renewable water (estimated in 2008), which is below the international water scarcity threshold of $1000\ \mathrm{m}^3\ \mathrm{inhabitant}^{-1}\ \mathrm{year}^{-1}$.

The United Nations Environment Programme (UNEP) 2010 Africa water atlas [1] lists "climate variability and water scarcity" and "public health concerns due to extensive dam construction" as the two main problems in Burkina Faso regarding water resources, related to erratic rainfall patterns and short rainy seasons. Before 1960, approximately 100 dams were built, but the majority was constructed in response to the droughts of the 1970s and 1980s. Many reservoirs are small and are subject to high evaporation rates of about 60% of the water [7]. 40% of the approximately 1400–2100 dams (numbers vary from source to source) in Burkina Faso have been built in the North where rainfall periods are short and erratic. These small reservoirs do not collect a sufficient amount of rain to sustain the water needs of the population. Due to strong population growth, those water needs continue to rise, and, therefore, new dams and reservoirs are created [1], [8]. Water availability in wetlands, reservoirs, and wells, as well as rainfall amount and distribution play an important role for farmers, herders, and fishermen for water supply to cities and villages and for electricity generation. This is most important during the dry season, from October to May/June.

In this work, the terms "wetlands" and "water bodies" will be used to refer areas flooded during at least 2 months per year. The focus lies on water availability, thus only the water-covered part, not the vegetated part, is considered. The surface area of the 20 largest wetlands after the rainy season is above $5\ \mathrm{km}^2$. Among them, Bagré is the largest wetland in the study area with about $175\ \mathrm{km}^2$, and three more wetlands are in the range of $50\ \mathrm{km}^2$. Small wetlands down to approximately $0.1\ \mathrm{km}^2$ were included in the analysis. Wetlands occurring in the study site are either natural or artificial wetlands, the latter created by man-made dams. Dams are built to create artificial wetlands, which serve as reservoirs and collect rainwater. Water abstraction is usually

Manuscript received December 18, 2013; revised May 19, 2014; accepted June 05, 2014. Date of publication August 10, 2014; date of current version October 03, 2014. This work was performed under the GIONET project supported by the European Commission, Marie Curie Programme, Initial Training Networks under Grant agreement PIT-GA-2010-264509.

L. Moser, S. Voigt, and E. Schoepfer are with the German Aerospace Center (DLR), German Remote Sensing Data Center (DFD), 82234 Wessling, Germany (e-mail: linda.moser@dlr.de; stefan.voigt@dlr.de; elisabeth.schoepfer@dlr.de).

S. Palmer is with the Balaton Limnological Institute, Hungarian Academy of Sciences Center for Ecological Research, 8237 Tihany, Hungary (e-mail: stephanie.palmer@okologia.mta.hu).

Color versions of one or more of the figures in this paper are available online at http://ieeexplore.ieee.org.

Digital Object Identifier 10.1109/JSTARS.2014.2336875

1939-1404 © 2014 IEEE. Translations and content mining are permitted for academic research only. Personal use is also permitted, but republication/redistribution requires IEEE permission. See http://www.ieee.org/publications_standards/publications/rights/index.html for more information.

performed for irrigation, water supply for cities, or electricity generation. Both artificial and natural wetlands fulfill certain ecosystem functions [9]: they are used as water reservoirs, important for water consumption, used for different livelihoods in the study area (agricultural, pastoral, fishery, domestic, and industrial use), serve as buffer for flooding, contribute to carbon sequestration, and are habitats for various species. Siltation, whereby fine sediment accumulates at the bottom of a lake, is causing wetlands to become shallower, which is considered to be the largest problem for all wetlands in Burkina Faso, particularly for natural wetlands.

A. Earth Observation for Monitoring Water and Wetlands in the Sahel Region

Remote sensing has the potential to play an important role for wetland monitoring [10]. Monitoring over such large areas can become a challenging task since temporal dynamics persist and regional and latitudinal differences occur. In this study, the Moderate Resolution Imaging Spectrometer (MODIS) sensor has been used to map water on a 250-m scale using the near-infrared (NIR) reflectance band [11], [12] making use of the strong absorption of NIR energy of water in contrast to land surfaces. Similarly, the normalized difference vegetation index (NDVI) serves to separate land and water [13]. Combined studies classify wetlands at 250-m scale using wet-season NIR metrics as a proxy for flooding and dry season NDVI metrics as a proxy for chlorophyll dynamics [11], [14]. At the 500-m scale, MODIS provides seven bands in the visual, NIR, and shortwave infrared (SWIR) range that allow the calculation of other indices applicable to water detection that use also bands in the blue and SWIR range. Other studies have used, e.g., the normalized difference water index (NDWI) and a modified NDWI (mNDWI) [15], land surface water index (LSWI), global vegetation moisture index (GVMI) [16], open water index (OWI) [17], and floating algae index (FAI) [18], [19]. The enhanced vegetation index (EVI) [20], which is used for calculation of some of the above-mentioned water indices, also serves for excluding vegetated areas. The above-listed indices have been successfully applied for surface water detection and monitoring, or flood detection from MODIS [21]–[25].

Presently, large Earth observation projects such as GlobWetland II to map Mediterranean wetlands on a high-resolution scale exist [26], [27], or TIGER-NET that supports satellite-based assessment and monitoring of water resources in Africa [28]. Other wetland studies focusing on the Sahel area, partially including Burkina Faso, provide monitoring or mapping of wetlands using MODIS 250 m data [11] and SPOT VEGETATION data of 1 km resolution. They are focusing on the seasonal behavior of water bodies [29], [30] where a positive relationship between rainfall anomalies and the area of temporary surface water bodies could be found [30]. On a high-resolution scale, the paradox of more rainfall but less water in the wetlands of certain areas in the Sahel is addressed with a multisensor approach [31]. Summarizing, the monitoring of Sahelian wetlands still remains a challenge due to spatial and temporal requirements to monitor small wetlands with strong seasonal differences.

B. Objectives

Despite the importance of water availability on livelihoods, existing knowledge and monitoring of wetlands are lacking. The number of natural and artificial water bodies, their surface areas and temporal dynamics, as well as the number of existing dams is not fully documented. Therefore, this work addresses spatiotemporal changes of the water coverage of wetlands derived from time series analysis of MODIS imagery, analyzing both seasonal patterns and inter-annual variability. The flooding regime (number of water covered months per year) variability in time and space between different years and different wetland types (natural or artificial), sizes and latitudes is explored. For demonstration, five case studies within the study area were selected, covering different lakes from the Sahel to the Sudano–Savannah region of Burkina Faso. The time-series analysis of surface water area shows the potential for novel early warning indicators of drought.

II. Study Area and Data

A. Study Area

The study area is located in the land-locked country of Burkina Faso, West Africa. A north–south transect extending to Mali in the North and Ghana in the South, with a width of approximately 200 km and a length of 500 km, was selected (Fig. 1). Flat terrain with an average elevation of 250 to 350 m above sea level dominates the region. All rivers are seasonal. The Volta catchment with the three main rivers, Nakambé, Mohoun, and Nazinon, extends through the central and southern part of the study area. The north-eastern part belongs to the Niger catchment. A strong gradient persists in terms of precipitation, ranging from less than 300 mm annual precipitation in the north to more than 1000 mm in the south. Three climatic zones are crossed from north to south: the Sahel region, Sudano–Sahelian *Savannah*, and Sudanian Savannah. Land use varies within different livelihood zones, where livelihoods are defined as "the means by which households obtain and maintain access to essential resources to ensure their immediate and long-term survival" [32]. In Burkina Faso, livelihoods are based mainly on farming and pastoral activities, which both strongly depend on the availability of water, particularly during the dry season, from In Burkina Faso, livelihoods are based mainly on farming and pastoral activities, which both strongly depend on the availability of water, particularly during the dry season, from October to May/June.

The northern part of the study region consists predominantly of a pastoral zone with transhumant pastoralism. Millet and cereals are found in the northeast, whereas in the central and southern parts, agricultural zones of cereals, sorghum, market gardening, fruits and cotton prevail [32]. Burkina Faso is considered to be a "hotspot" of water-constrained, rain-fed agriculture, related to effects of climate change on food security. Water distribution is anthropogenically influenced by the construction of about 1400 to 2100 dams across the country. Although data are not available for the majority of the dams, according to visual interpretation of high-resolution satellite imagery, these tend to be on the order of several

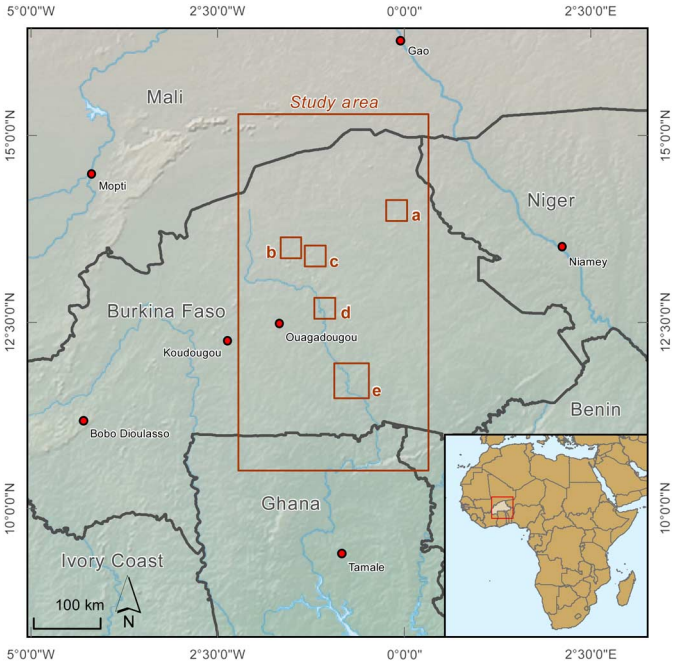

Fig. 1. Study area, located in Burkina Faso, West Africa, marked with the large rectangle. The five wetland cast studies (a)–(e) are displayed as small rectangles: (a) Barrage de Yakouta (a); (b) Lac Bam; (c) Lac Dem; (d) Barrage de Ziga; and (e) Barrage de Bagré.

hundred meters to more than 1 km in length. The few largest dams in the study area are of more than 4 km in length. Many of them are used mainly for small-scale irrigation [1], e.g., of rice and vegetables, although most of Burkina Faso's agriculture is rain-fed. The country is ranked 183rd out of 187 countries in the human development index (HDI) [33]. Burkina Faso has a population of approximately 16 million people, and strong population growth of about 3% per year has been reported [34].

Five wetlands were selected as case studies for detailed analysis according to different criteria, such as reasonable size for monitoring with MODIS pixel resolution, geographic distribution from north to south, differences in type (natural or artificial), and international importance as described by the RAMSAR Convention on Wetlands of International Importance, founded in 1971 [35]. The case studies from north to south are further described as follows.

La Barrage de Yakouta (site a) is a new artificial lake with a surface area (the area covered by water two or more months per year) of approximately $10.5\ \mathrm{km}^2$ that was formed along a river between 2004 and 2005 after dam construction in Burkina Faso's northern Sahel region, close to the village Yakouta. This event is apparent in the time-series analysis as shown in Section IV (Fig. 8). The purpose of this reservoir is to provide water to the city of Dori located about 10 km to the east. It is otherwise used by herders, and some fishing and small irrigation activities also take place. *Lac Bam* (site b) is the largest permanent natural lake (about $23.5\,\mathrm{km}^2$) in Burkina Faso, and as such a RAMSAR site. Water abstraction is performed solely for irrigation. Other anthropogenic activities include fishing, livestock breeding, and subsistence and cultivation farming for export. Siltation is a major concern. Increasing land use activities such as irrigated cultivation cause deforestation and conversion from naturally vegetated land into cultivated land, which foster sediment input into the lake. The lake is highly important for various animal species, particularly fish [7]. *Lac Dem* (site c) is a permanent natural lake and a RAMSAR site of about $6\,\mathrm{km}^2$. Water is abstracted for irrigation and for water supply of the provincial capital city, Kaya, located nearby. Irrigated cultivation poses a threat due to pesticide use and water removal. Water scarcity may force livestock routes to change, and conflict between farmers and herders occasionally occurs. Likewise, similar to Lac Bam, it is strongly prone to siltation. Over-fishing due to both population pressure and climate change has resulted in the extinction of various terrestrial and aquatic species [35]. A large, permanent, artificial lake, *la Barrage de Ziga* (site d), is located 50 km from the capital city, Ouagadougou, and has a surface area of approximately $58\,\mathrm{km}^2$. The dam was built on the Nakambé River between 1998 and 2000 to secure the availability of freshwater resources for the city of Ouagadougou, providing a near continuous water supply [36], [37]. Further south, *la Barrage de Bagré* (site e) is a permanent artificial lake created by a large dam built in 1992 on the Nakambé River in southeastern Burkina Faso. It is the largest wetland in the study area (about $175\,\mathrm{km}^2$) and is a RAMSAR site. Water from the reservoir is abstracted for the irrigation of large areas, mainly rice fields to the South of the dam, and for electricity generation. The construction of dams might influence downstream hydrological characteristics. In the Nakambé catchment, 242 dams have been built until 2005 [38]. Bagré and Ziga as well as the two natural wetlands Bam and Dem are located in the Nakambé catchment. It was found that since the 1960s, the hydrological regime of the Nakambé River has changed due to the construction of many dams. Despite rainfall having decreased and the number of dams increased, average runoff and maximum daily discharge increased. Therefore, the hypothesis that increasing land use may lead to higher runoff in rivers is supported [38].

To summarize, from the five case studies, only Barrage de Bagré is used for electricity generation; Barrage de Ziga, Lac Dem, and Barrage de Yakouta are used for water supply to towns; and all water bodies besides Barrage de Ziga for irrigation. In the case of Bagré, large rice fields are irrigated, in contrast to the small fields belonging to different villages and farmers which are more typical throughout the country.

B. Data

MODIS surface reflectance data at 250 m resolution (MOD09Q1) and at 500 m resolution (MOD09A1) were used to generate a time series between the years 2000 and 2012, with a temporal frequency of 8 days. The MOD09Q1 product is a Level-3 surface spectral reflectance product, precisely geolocated and composited over 8-day intervals. It consists of two 250 m spatial resolution bands, band 1 corresponding to the red spectral range (620–670 nm) and band 2 to the NIR range (841–876 nm), and an additional band quality layer. In the compositing process, the best observation over an 8-day period is selected for each pixel based on MODIS level-2 products, according to criteria such as cloud-free and cloud

shadow-free observations, aerosol loading, high observation coverage, or low viewing angle. The MOD09A1 product is produced similarly to MOD09Q1, but contains seven 500 m spatial resolution bands spanning the visible, NIR, and SWIR range, and includes state flags and quality information [39], [40]. MODIS data are available in Sinusoidal projection and were provided by Reverb of the National Aeronautics and Space Administration (NASA) Earth Observing Data and Information System (EOSDIS).

The Digital Elevation Model (DEM) from the Shuttle Radar Topographic Mission (SRTM) flown by the (NASA) in 2000 was used. This DEM has been derived by interferometric techniques using two SAR antennas onboard the Space Shuttle and is available globally between $60°$ North and $54°$ South with a spatial resolution of 90 m [41], [42]. In order to verify water-covered pixels in MODIS data, and consequently to define suitable threshold values, bi-seasonal Landsat images were used from two different years. Three Landsat images (path 194, rows 50, 51, and 52) from February 16 2002, acquired by the Landsat 7 Enhanced Thematic Mapper (ETM+), were selected to serve as dry season reference. For the end of the rainy season reference, eight Landsat 5 Thematic Mapper (TM) images from September 23, 2009 (path 194, rows 50, 51, and 52), October 9, 2009 (path 194, rows 50, 51, and 52), and October 16, 2009 (path 195, rows 50, and 51) were chosen.

III. Methodology

Fig. 2 shows the processing chain implemented in IDL8.2 including 1) the input data; 2) intermediate processing steps; 3) water masks; and 4) derived products for categorization, spatiotemporal analysis and the retrieval of time series information.

A. Water Mask Processing Chain

MODIS 8-day composite NIR surface reflectance values from February 2000 to December 2012 were imported in order to form image stacks and time series. The 500 m state flags were also imported and resampled to the higher MODIS pixel resolution. Cloud removal and removal of bad quality pixels were performed using the resampled 500 m state flags, the band quality information and additional thresholding on the reflectance bands. Thereafter, 8-day NIR composites were aggregated to monthly averaged values.

A per pixel quality mask was created containing the number of valid observations that were used to build the monthly averaged images. Pixels with no valid observations were flagged. The SRTM DEM preprocessing included the reprojection to Sinusoidal MODIS projection, resampling and coregistration to the MODIS pixel size and subsetting to the area of interest (AOI) extent. Slope inclination in degrees was then calculated. The whole terrain is characterized by very flat topography, apart from some rock outcrops with steep slopes and plateaus on top. Shadows related to these slopes were removed by building a topographic shadow mask.

Surface water mapping was carried out via a thresholding approach using the NIR band, since water strongly absorbs

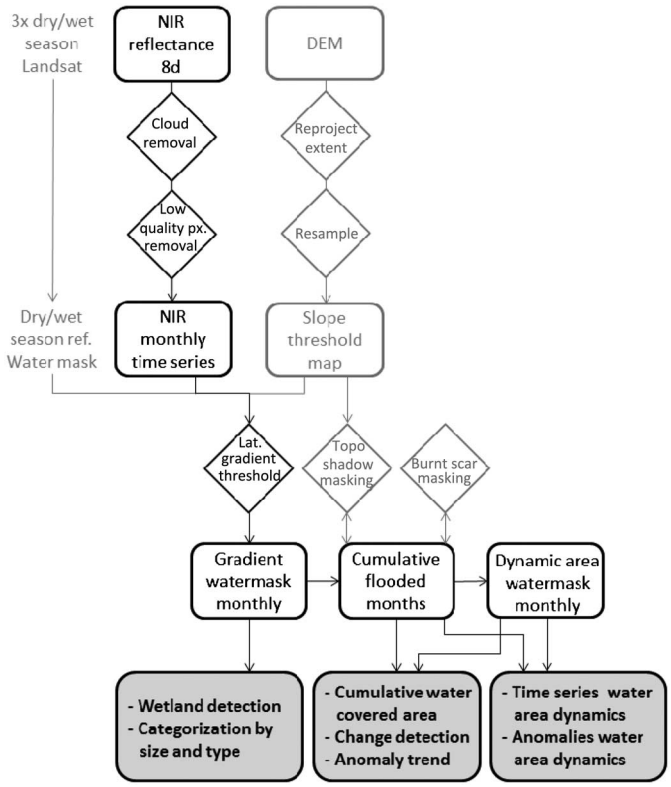

Fig. 2. Overview of the processing chain showing the main input data: NIR reflectance (black) and SRTM DEM (gray), followed by intermediate processing steps, water mask generation and highlighting retrieved products for categorization, spatiotemporal analysis, and creation of time series information.

light in the NIR spectral region leading to low reflectance in NIR bands, in contrast to the higher NIR reflectance of land surfaces. In order to derive an appropriate mean water threshold for the given region, three selected dry and wet season Landsat images were used. The images were selected to verify water-covered areas on a higher resolution scale by applying a NIR threshold and calculating NDWI. A total of 30 samples of water-covered AOIs were chosen across different latitudes, covering various wetlands bi-seasonally. Adjacent pixels within a minimum radius of 250 m around the AOIs were required to be covered with water in order for a pixel to be included within the water-covered AOI. Corresponding NIR surface reflectance values were measured in the MODIS data. First, thresholding trials revealed that due to regional differences along the north-south transect, variations within the same water body, and seasonal differences between the rainy and dry seasons, no single threshold value was suitable. NIR reflectance values are up to 5%–10% higher in the dry season as compared to the rainy season, because the sediment rich water causes a stronger reflectance in the visible wavelengths, which, however, slightly affects the NIR as well. Predominantly artificial water bodies, located in the center and southern parts, were well detected using a lower reflectance thresholds, around 15% surface reflectance at the end the of the rainy season, whereas natural wetlands in the north of the study area could only be mapped using higher thresholds, in the range of 25%. Therefore, a latitudinal gradient NIR

threshold ranging from 15% (10°N) to 25% (15.5°N) was applied. The gradient is a consequence of the characteristics of the water bodies in the study area along a transect covering three different climatic zones, rather than a general function of latitude itself. Moreover, the DEM derived slope inclination was used as a further condition of exclusion to retrieve the water masks. Any value exceeding a threshold of 1° of slope inclination was excluded, in order to rule out shadows caused by steep slopes. For every month in the time series, a water mask was calculated.

Three validation sites at different locations along the transect were chosen: Barrage de Yakouta in the north, Lac Bam in the centre, and Barrage de Bagré in the south. The MODIS water mask for October 2009 serves as a basis for validation. Five Landsat images from October 9 (path 194, rows 50, 51, and 52), and October 16 (path 195, rows 50 and 51) 2009 serve to 1) create a water mask based on NDWI thresholding; and 2) digitize the open water surface including the floating or standing vegetation. The finer spatial resolution of Landsat (30 m) allows the validation of MODIS water masks, as seen in Fig. 5.

B. Spatiotemporal Analysis of Water Mask-Derived Products

Wetland detection and categorization by size and by natural/artificial type was carried out by calculating areal statistics using ArcGIS10.1. Surface water dynamics were derived by summing the monthly calculated water masks into cumulative water covered months per year. This step was performed for each hydrological season over the period 2000–2012, starting with the beginning of the rainy season in May and ending at the end of the dry season in April of the following year. On one hand, this indicates the extent of the area covered by water, and on the other hand, it shows the temporal aspect in terms of number of water covered months per pixel for each season (Figs. 3 and 7). Regularly appearing phenomena that could be misclassified as water, such as topographic shadows or bushfire scars were masked out. Topographic shadows always appeared in the same spot, and could be masked out by using the DEM, whereas burn scars were only visible for a couple of days to weeks and in most cases were masked out by the definition that only pixels covered by water masks for minimum two months per year are counted as wetlands.

The cumulative water-covered area was used to distinguish between the permanent and dynamic areas of each wetland. A near-permanent region was defined by greater than or equal to 9 months of water coverage, considering known errors in the water masks due to masked out pixels resulting from cloud cover during the rainy season. As a result, the dynamic region is covered by water between 1 and 8 months. Change detection between a water mask from 2000 and 2012 was carried out (Fig. 6). All pixels covered by water between 2 and 12 months per year were considered for the masks, and the water mask of the year 2000 was subtracted from 2012. In order to separate new or vanished water pixels due to yearly varying size changes from the desired newly appeared or totally vanished water bodies, the wetland masks of the year 2000 and 2001 were compared with the ones of 2011 and 2012. Thereafter, a standardized anomaly trend was calculated from the per-pixel anomalies of the cumulative the cumulative water-covered area (Fig. 7). This is defined by the per pixel linear regression through the deviation from the mean of cumulative water-covered areas, divided by the standard deviation of the cumulative water-covered area of the respective year.

C. Surface Water Area Time Series

Five case studies were chosen to derive the temporal dynamics of water-covered areas from the time series. Therefore, time series of water-covered areas were converted from number of pixels to area (in square kilometers) and to relative values (in percent), with 100% being the time series' maximum (Fig. 8). Monthly water-extent area in square kilometers was compiled as ASCII sequential data. The areas served as input into the TIMESAT software [43], [44] and all implemented smoothing functions were applied. The Gaussian fit proved to be the best fitting function, through comparison of chi square goodness-of-fit with the input time series. Surface water area anomalies, calculated as the deviation from the 13-year mean of each respective month, were calculated. The focus lies solely on the dry season beginning with the peak value (around October–November) at the end of the rainy season until the end of the dry season (around May). Due to the frequent occurrence of cloud cover, mostly in July and August as well as in June and September, data during the rainy season were assumed not to be reliable. Therefore, these 4 months were excluded from the time series analysis of surface water areas anomalies (Fig. 9).

A field survey in Burkina Faso was carried out from October to November 2013 for better understanding of the local context, carrying out interviews with the local population and representatives from local institutions, and gathering reference information in the field. The focus of the expert talks was regarding the occurrence and timing of drought periods and reduced water levels and water areas.

IV. Results

A. Wetland Detection and Categorization

The study area has been divided into northern, central and southern regions. Following the definition that a wetland is an area covered by water in a minimum of 2 monthly composites per year, categories of size, natural/artificial type and distribution of wetlands have been compiled in Table I. Size was calculated as the maximum area covered by water for at least 2 months per year, in all of the 13 years of the study period. 219 wetlands with a spatial extent greater than $0.1\,\mathrm{km}^2$ were detected, among them 68 are larger than $1\,\mathrm{km}^2$. 35% of the wetlands larger than $0.1\,\mathrm{km}^2$ are situated in the northern part of the study area, 57% in the central part and 8% in the south. The majority of wetlands are located in the central part, being an area with substantial agricultural activities and on the southern edge of the pastoral zone. It can be observed that in the northern and north-eastern pastoral zone, natural wetlands are predominant. Going furthersouth, anthropogenic influence

TABLE I
WETLANDS OF THE STUDY AREA CLASSIFIED BY SIZE, TYPE, AND SITE

Region	# of total > 0.1 km^2	# of natural > 1 km^2	# of artificial > 1 km^2	> 50 km^2	> 5 km^2	> 2 km^2	> 1 km^2	> 0.5 km^2	> 0.1 km^2
North	**76**	22	10	0	9	15	8	10	34
Centre	**125**	4	28	2	7	9	14	25	68
South	**18**	0	4	1	1	1	1	1	13
TOTAL	**219**	26	42	**3**	**17**	**25**	**23**	**36**	**115**

becomes more obvious, as agricultural activities increase and no natural wetlands appear. The lowest density of wetlands is observed in the south, which is dominated by the largest water body in the region, la Barrage de Bagré, and two artificial water bodies in north-Ghana.

The largest water body, la Barrage de Bagré, has a surface area of approximately $175\,\mathrm{km}^2$ and is followed in a real extent by Barrage de Ziga covering slightly more than $50\,\mathrm{km}^2$. The largest natural lake is Lac Bam with approximately $23.3\ \mathrm{km}^2$ water surface area. Table I gives an overview of wetlands in the study area by size ($\mathrm{very\ large} > 50\ \mathrm{km}^2$, $\mathrm{large} > 5\ \mathrm{km}^2$, medium-large $> 2\ \mathrm{km}^2$, $\mathrm{medium} > 1\ \mathrm{km}^2$, medium-small $> 0.5\ \mathrm{km}^2$, $\mathrm{small} > 0.1\ \mathrm{km}^2$) in the northern, central, and southern region. Additionally, the wetlands are categorized into natural versus artificial wetlands.

In order to provide information on the minimum size of water bodies that can be captured with MODIS, an analysis has been carried out considering five Landsat images from October 9 (path 194, rows 50 and 52), and October 16 (path 195, row 51) 2009, at the end of the rainy season. The cumulative water-covered surface area for the year 2009–2010 (as shown in Figs. 3 and 7) is the basis for identifying the smallest detected wetlands (one MODIS pixel classified as being water covered for a minimum of two months per year). The area is subsequently measured from the Landsat images, for a sample of 30 small water bodies equally distributed over the study area. The average area of the measured small water bodies serves as an indication of the maximum size of the smallest water bodies that are still included in the analysis, which is on average $0.16\,\mathrm{km}^2$. This depends on the location of the mixed land–water pixels detected by MODIS, as well as the length to width ratio of the water bodies, which tend to decrease in area throughout the dry season.

B. Spatiotemporal Surface Water Dynamics

Surface water dynamics for the five wetland case studies are analyzed, focusing on the drought seasons. The seasons 2000–2001, 2004–2005, and 2011–2012 have been described as years of drought in Reliefweb [5] and 16 expert interviews with local institutions and villagers, who independently and consistently mentioned these seasons. The EM-DAT database [45] reports that the years 2000–2001 and 2011–2012 are having disastrous drought seasons. The drought season 2004–2005 is not mentioned for Burkina Faso in particular, but is for neighboring Niger, and will therefore be considered as well.

Fig. 3 shows the surface water dynamics as cumulative water-covered area, calculated as the number of water covered months for each year, using the large, artificial lake Barrage de Bagré (site e) as an example. Throughout the paper a year is considered to be from May to April of the following year, in other words from the start of the dry season to the end of the following wet season. Pixels colored in shades of blue are water covered throughout almost all the year, which corresponds to what was defined as near-permanent area, with water coverage between 9 and 12 months per year. Shades of green indicate the dynamic area, covered between 1 and 8 months per year.

From the five selected case studies, Bagré displays the largest seasonal variation between the dry and rainy seasons every year. As well as in area and width, the water body decreased significantly in length at the northern extent during the three periods of drought. In total, the maximum surface area associated with the drought seasons is considerably smaller than during nondrought years. The number of near-permanent area pixels, however, is found to be similar in drought and nondrought years. Although it is lower than average during the 2011–2012 drought year, this is not the case for 2000–2001 and 2004–2005, and some nondrought years are characterized by a lower than average permanent area. The dynamic area shows greater variability and is considerably smaller during the drought seasons. In the case of Bagré, an overall tendency toward a larger dynamic area is observed during the second half of the study period (Fig. 4).

In this analysis, it was revealed that Barrage de Yakouta (site a) did not yet exist at the beginning of the study period, and started to appear in the satellite images of the 2004–2005 season. It is a northern artificial wetland with a recently constructed dam intended to enhance irrigation and water supply in the Sahelian area. Yakouta is situated in an area of strong agricultural use, close to the towns of Yakouta and Dori. Nearby, there are two natural wetlands: Djigo in the north and Mar de Dori in the east. The first displays variation in size and in number of flooded months, whereas the second is not visible in most years, which can be explained by both high vegetation cover during and after the rainy season which prevents water detection from NIR bands, as well as drying out in the dry season. Seasonal and interannual variations are not as pronounced in Lac Dem (site b) and Lac Bam (site c) as for the other sites. However, the years 2004–2005 and 2011–2012 show less surface water extent for both lakes, and 2000–2001 shows less surface water extent just for Lac Dem. A decrease in flooding duration of Lac Bam's central area become evident, as well as similar variations in Lac Bam-2,

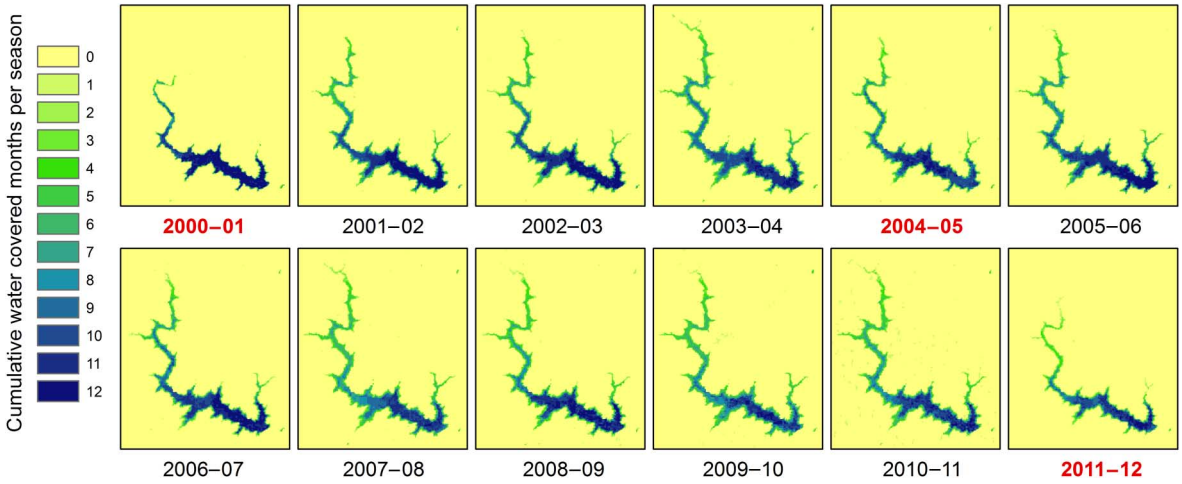

Fig. 3. Surface water dynamics of Barrage de Bagré (site e), displayed as cumulative water-covered surface area, from season 2000–2001 to 2011–2012. Drought seasons are marked in red (bold in B/W version).

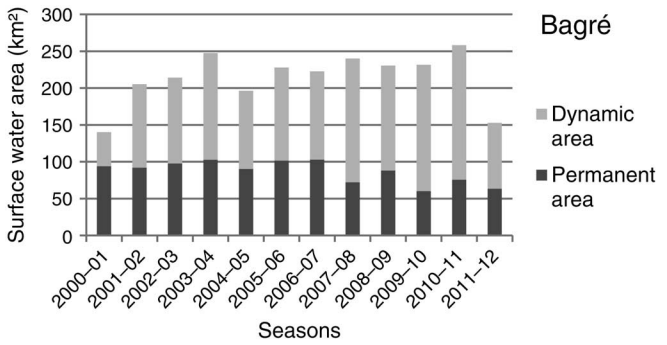

Fig. 4. Temporal development of near-permanent and dynamic area for Barrage de Bagré (site e), from season 2000–2001 until 2011–2012.

its neighbor which is situated 4.5 km to the west. Lac Dem's neighboring wetland to the north shows a clear reduction of water in the seasons 2000–2001 and 2011–2012. Since the construction of the Ziga dam (site d) along the Nakambé River was just completed in 2000, water coverage was low in area and duration for the year 2000–2001. In 2004–2005, a smaller maximum surface area and fewer near-permanent area pixels are observed in the northern part of the wetland. In 2011–2012, the surface area was significantly smaller and the permanent area along the upstream part was strongly reduced. Additionally, it becomes obvious that two new small water bodies appeared during 2005–2006, on either side of Barrage de Ziga.

Results of the validation of water extent for October 2009, carried out using Landsat imagery, show that in all three cases the MODIS surface water area was slightly underestimated with respect to the water area derived from the Landsat imagery, but showed results with a reliable accuracy in terms of matching the Landsat surface area with 93.5% (Barrage de Bagré), 92.4% (Lac Bam), and 89.5% (Barrage de Yakouta) as stated in Table II. Lac Bam is partially subjected to the presence of standing and floating vegetation that was not detected in either the MODIS or the Landsat water mask. When digitizing the water surface, including the vegetated

TABLE II
ACCURACY OF THE OCTOBER 2009 WATER MASK FROM THE MONTHLY MODIS COMPOSITE COMPARED TO A WATER MASK DERIVED FROM LANDSAT TM ON 9TH OCTOBER FOR (A) YAKOUTA, (B) BAM, AND (C) BAGRÉ

Region	MODIS (km²)	Landsat TM (km²)	MODIS % of Landsat TM (%)
Yakouta	12.8	14.3	89.5
Bam	20.6	22.3	92.4
Bagré	215.8	230.8	93.5

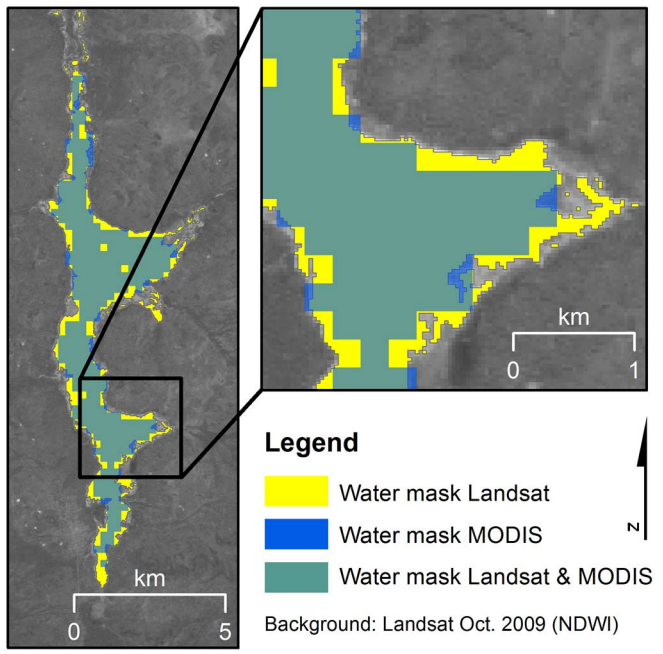

Fig. 5. Water masks of Lac Bam from October 2009, derived by Landsat NDWI threshold [yellow (light gray in B/W version)], overlaid with the water mask from the October 2009 MODIS NIR time series composite [blue (dark gray in B/W version)], showing overlapping regions in green (medium gray in B/W version).

parts, the resulting accuracy was 75.7%. Due to strong seasonal dynamics, however, the water surface calculated from the single-date Landsat image cannot strictly be compared

with a MODIS monthly composite, and can serve only as an approximation. Fig. 5 shows a comparative illustration of water masks derived from Landsat TM images and MODIS composites of October 2009.

A postclassification change detection was applied between the first (2000) and last (2012) years of the study period. As shown in Fig. 6, the occurrence of water pixels only in 2012 (blue) or only in 2000 (orange) indicates new or no longer existing water bodies, respectively. Gray color indicates that no change has taken place (pixels are either water covered in both years or were not water covered in either). Due to yearly dynamics, there are changes in the size of many wetlands from season to season. It must be considered that both the first and the last year of the study period experienced droughts, and can thus be considered anomalous. After the elimination of change pixels caused by size changes of water bodies, the remaining water bodies are marked with black boxes (new) and orange boxes (no longer existing).

In total, 21 new water bodies, each with a surface area of more than $0.5\ \mathrm{km}^2$, were found to have appeared between 2000 and 2012, and only a few small water bodies are found to have vanished. The previously discussed case studies Barrage de Yakouta (a), built during the study period, and Barrage de Ziga (d), in the final construction phase at the beginning of the study period, show up in blue (Fig. 6). Ziga (d) increased substantially in water surface but is not counted as a new water body since dam constructions were ongoing in 2000 and the water body already existed with smaller water extent.

The three most significant new water bodies are highlighted in Fig. 6(f), (h), and (i). During expert interviews in the field, it was revealed that the water bodies (f) and (h) were not created as reservoirs for water supply or irrigation, but for gold mining by large by large international companies. Two sites seem to have disappeared: a small water body in the north-east of Lac Bam [Fig. 6(g)], and three smaller wetlands [Fig. 6(j)] to the south-east of the capital, Ouagadougou. The Ouagadougou. The reason might be disrupted dam performance due to floods, poor maintenance or destruction, causing the reservoir to dry out. Orange pixels in the west of Bagré are misclassifications caused by burn scars that did not persist long enough to be masked out.

The cumulative water-covered area of the entire study region from all seasons from 2000–2001 to 2011–2012, with pixel values between 0 (never water covered) and 12 (all season water covered) was used as input to calculate a standardized anomaly trend (Fig. 7). Positive trends can be interpreted as a trend toward longer water coverage per season, and negative trends toward fewer months of water coverage. toward fewer months of water coverage. Fig. 7 shows the trend of anomalies for the entire study area and highlights the five case water coverage per season on the left. Positive and negative trends are spread along all latitudes of the study area. Barrage de Yakouta (a) and Ziga (d) show a positive anomaly trend due to dam construction as previously discussed. New water bodies, as discovered in the change detection, such as sites f and h, logically reveal to a very positive trend. However, site i, which did not exist prior to 2012, does not show up in the trend

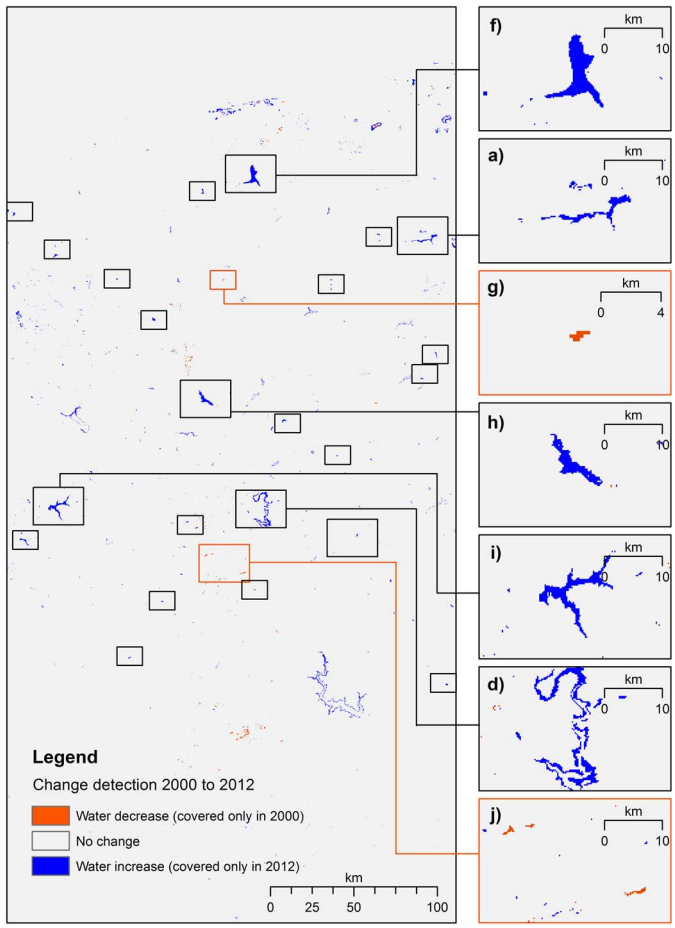

Fig. 6. New water bodies [blue (white in B/W version)] and vanished water bodies [orange (black in B/W version)] as detected in the postclassification change detection between 2000 and 2012. Examples are shown in black (gray in B/W version) zoom-boxes (new wetlands) and orange (black in B/W version) zoom-boxes (vanished wetlands).

analysis considering only the time period until the end of the season 2011–2012. Strong negative trends are observed for Lac Bam (b) and for the natural wetland Bourzanga to the north of Lac Bam. Lac Dem [Fig. 7(c)] shows a partially negative trend but a positive trend on its eastern coast. A slightly negative or no trend are observed for the central part of Barrage de Bagré (e), surrounded by a zone of negative trending area followed by an extreme outer zone of positive trending pixels.

Expert interviews in the field revealed that siltation causes the lake to become shallower, but also forces the water to spread out more in surface area. As documented in Fig. 4, a larger dynamic area over the past couple of years has become visible for Barrage de Bagré. This may explain the positive trend of the extreme outer pixels and the negative trend on adjacent pixels inside this. On one hand, spreading to larger water extents occurs at the cost of reduced duration of water coverage in the more central areas, and on the other hand faster retreat of shallow water due to evaporation takes place. Additionally, Sonabel, the company operating the dam, reported that it had repeatedly filled the reservoir to its maximum capacity overthe past years (2003, 2007, 2008,

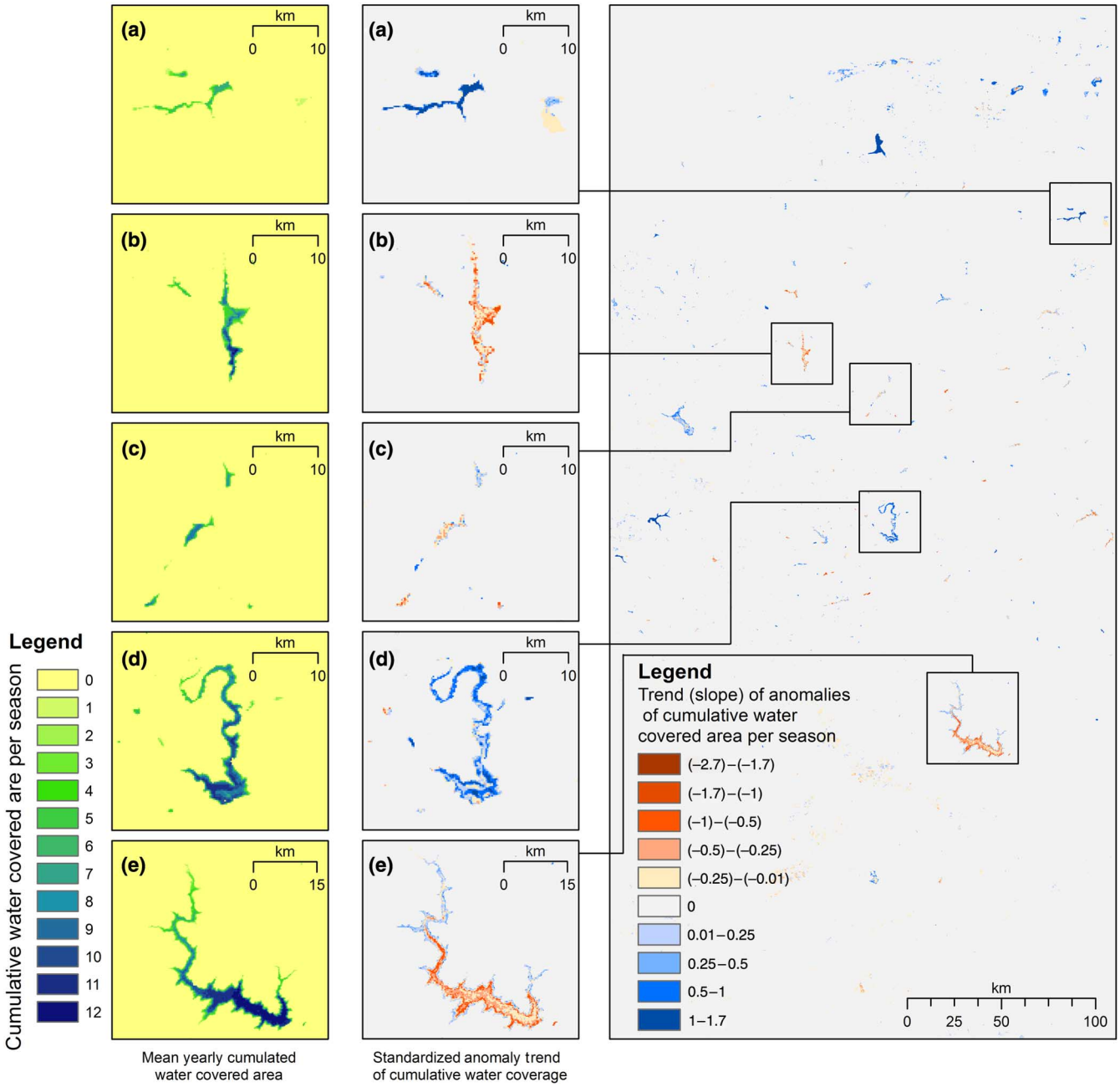

Fig. 7. Left: Mean cumulative water-covered area over 12 seasons for the case studies: (a) Yakouta; (b) Lac Bam; (c) Lac Dem; (d) Ziga; and (e) Bagré. Right: Anomaly trend of cumulative water-covered area (2000–2001 to 2011–2012). Negative trend values [red (dark gray to black in B/W version)] signalize a negative trend and positive values [blue (light gray to white in B/W version)] a positive trend.

2009, 2010, and 2012) [46]. Although less pronounced, a similar negative trend in the central part of a wetland and positive trend at the outer limits can also be detected for the eastern coast of the natural wetlands Lac Dem (c), Lac Bam (b), the aforementioned Bourzanga and Lac Bam-2, as well as on several artificial water bodies along the east of the study area.

C. Temporal Dynamics of Water-Covered Areas

A time series of the water-covered surface area is visualized to explore the trend analysis (Fig. 8). When and to what extent changes in the wetland temporal dynamics take place are analyzed by plotting monthly time series of the water-covered area in km^2 per wetland. For each of the five case studies (a–e), time-series smoothing was carried out using a Gaussian asymmetric fit. The values were rescaled to relative values in percentage (0%–100%), with 100% defined as the maximum water area of the maximum year of each respective wetland.

Fig. 8 shows the three artificial wetlands of the five case studies (a, d, e; above) and the two natural wetlands (b, c; below). It is observed that natural as well as artificial wetlands have a distinct annual cycle, demonstrating a

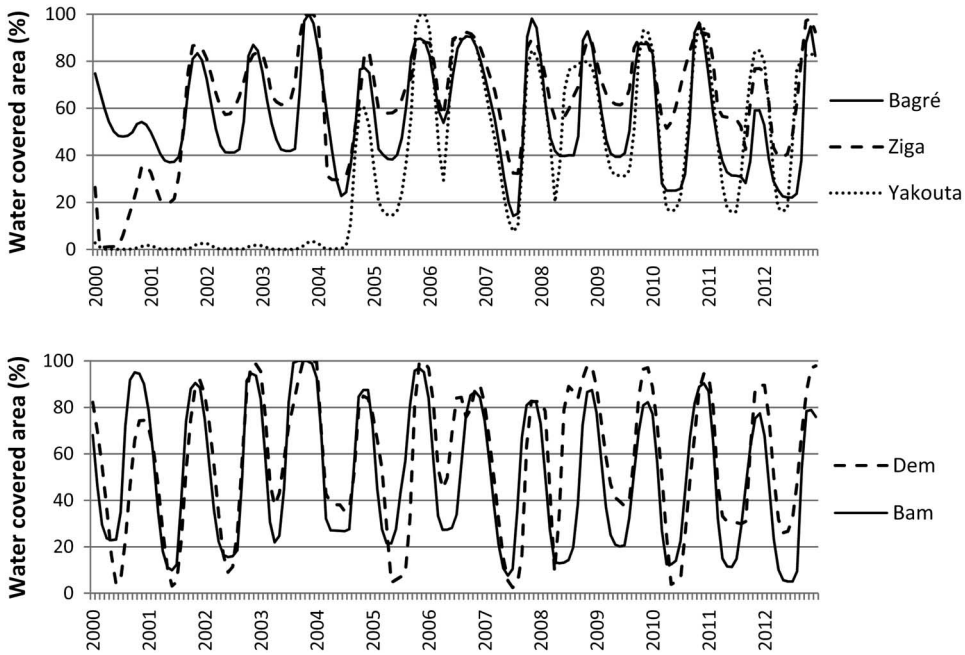

Fig. 8. Above: Three artificial wetlands: Barrage de Bagré (e) solid line; Barrage de Ziga (d) dashed line; and Barrage de Yakouta (a) dotted line. Below: Two natural wetlands: Lac Dem (c) dashed line and Lac Bam (b) solid line.

characteristic seasonality with regards to their monthly water-covered area in square kilometers. The two natural wetlands, Lac Dem and Lac Bam, appear to have a more regular seasonal cycle. One might assume that the cycle of the reservoirs regulated by dams would be more irregular due to rapid output of water to meet the needs of water supply to towns, irrigation, or industry. However, during expert interviews in the field and with local institutions, it has been found that water removal is done quite regularly and that there is no such rapid overspill of water. The only exception is in the case of exception is in the case of large dams when maximum reservoir capacity is reached [46]. Fig. 8 shows that both Barrage de Bagré and Barrage de Ziga reached their maximum surface water area at the end of the 2003 rainy season, followed by the lowest water extent peak in the 2004–2005 and 2011–2012 seasons, the latter notably so for Bagré. The time series clearly reveals the effect of the newly built Yakouta dam in the middle of 2004, demonstrating the potential of retrieving dam construction timing from MODIS imagery. Yakouta reaches its maximum water extent at the end of the rainy season 2005, the year following its construction. It is observed that both Bagré and Yakouta display larger relative variation in water extent throughout the year than does Ziga. The two natural wetlands Lac Bam and Lac Dem reach their lowest peak values in 2000–2001, 2004–2005, and 2007–2008, and in the case of Lac Bam also 2011–2012.

Fig. 9 displays the areal extent (km^2) anomalies of each month relative to the mean of the same month from the entire study period (2000–2012) for all five selected case studies, from north to south. Only the dry season, from October to May, has been considered for the anomaly analysis, due to too many missing data values during the rainy season caused by cloud cover. Seasons where more than 2 months had a negative anomaly, are shaded in gray. The anomalies of the Yakouta reservoir (a) are only considered starting in October 2005 after construction of the dam. Values before that date are not considered for calculation of mean and anomaly. Anomalies are in the range of $-2\ \mathrm{km}^2$ to $+2\ \mathrm{km}^2$ with the exception of the season 2005–2006 reaching almost $+5\ \mathrm{km}^2$. All other seasons display positive as well as negative anomalies throughout the season, from i2006–2007 to 2008–2009 the season begins with more negative anomalies and ends with positive anomalies. However, from 2009–2010 to 2011–2012 negative anomalies dominate the end of the dry season for all years. Lac Bam (b) shows greater anomaly variability, between $-6\ \mathrm{km}^2$ and $+6\ \mathrm{km}^2$, high positive values are reached at the end of the rainy season in 2003 and 2005, and in the middle of the 2010–2011season, and low anomalies occur in the 2000–2001 and 2004–2005 seasons, slightly in 2007–2008, 2009–2010 and particularly strong in 2011–2012. Anomalies of Lac Dem (c) are in the range of $-2\ \mathrm{km}^2$ to $+2\ \mathrm{km}^2$, negative as well as positive anomalies occur throughout the whole time span. Lowest anomalies are seen in the 2000–2001, 2004–2005, 2007–2008, 2009–2010, and 2011–2012 seasons. Anomalies of Barrage de Ziga (d) are in the range of $-15\ \mathrm{km}^2$ to $+20\ \mathrm{km}^2$, excluding the year 2000–2001 during which anomalies as low as almost $-30\ \mathrm{km}^2$ occur, which are suspected to relate to the final stage of dam construction. Only positive anomalies are found from 2005–2006i to 2010–2011, negative anomalies in the dry season 2004, and 2004–2005 and 2011–2012 seasons. The absolute anomalies for Barrage de Bagré (e) are much larger than for Barrage de Ziga, and range between $-65\ \mathrm{km}^2$ and $+55\ \mathrm{km}^2$. Positive anomalies are observed in all years except in 2004–2005 and 2011–2012,

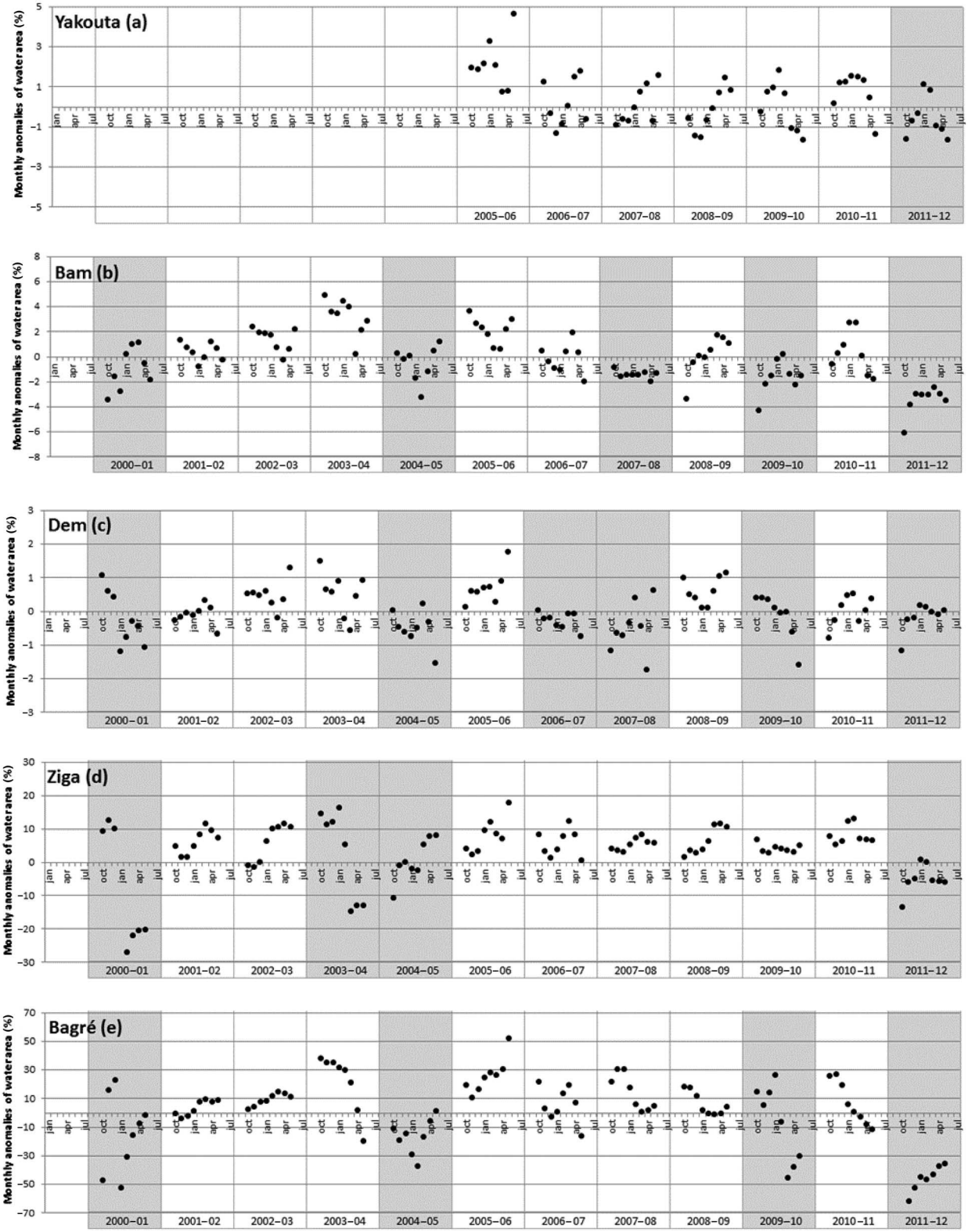

Fig. 9. Monthly anomalies with respect to the 13-year mean of each month, displayed for the dry season (October–May) 2000–2001 to 2011–2012 for the five case studies from north to south: (a) Yakouta; (b) Lac Bam; (c) Lac Dem; (d) Ziga; and (e) Bagré. Seasons with significant negative anomalies are shaded gray.

consisting of negative anomalies alone. The largest positive anomalies are found during the 2003–2004 and 2005–2006 seasons.

In summary, the seasons 2000–2001, 2004–2005, and 2011–2012 are significant throughout the study area, with low maximum surface water area levels and negative anomalies

in all studied wetlands. This corresponds with the seasons reported to be drought years. The seasons 2003–2004 and 2005–2006 show largest positive anomalies across all wetlands.

V. Discussion

The NIR-based water detection using a latitudinal threshold gradient approach, as described in the Methodology section, performed well in the southern and central areas of the study area, where larger water bodies and artificial reservoirs with dams are predominant. The study remained challenging in the northern part, characterized by natural water bodies of smaller size, and which are frequently covered by floating vegetation or standing vegetation part of the year, or might completely dry out toward the end of the dry season (around April–May). In order to improve the water detection and surface wetness detection in northern vegetated wetlands, the MOD09A1 product could be used. The product offers seven bands. Two bands are in the SWIR range and two in the visible range (blue, green) at 500 m resolution, which can be used for exploitation of further water indices [21]–[24]. This is recommended in addition to the use of the 250 m NIR band, used in this study, so as to not decrease the spatial resolution. The cumulative water-covered surface area was frequently underestimated in northern wetlands as a result of floating vegetation coverage. Due to the wetland definition of a minimum of 2 months water coverage per year, one larger wetland in the north, Mar de Dori, was excluded from the analysis. Satellite data at medium resolution, such as MODIS, are subject to mixed pixels at shorelines, and in the case of floating vegetation cover or standing vegetation in the water body.

Remote sensing satellites currently in orbit, such as RapidEye, Landsat-8 and DMCii, or the future Sentinel-2 acquire high spatial resolution imagery with frequent time steps and therefore show great potential for water detection which is less prone to mixed water-vegetation pixels due to their higher spatial resolution. In this work, only wetlands greater than $0.1\ \mathrm{km}^2$ surface water area were considered. For the observation of smaller wetlands, which are likely to be even more sensitive to climate fluctuations, higher resolution satellite data is needed. This has been demonstrated in various studies [31], [47], [48]. However, data from these satellites are not acquired with such a high temporal frequency, spatial coverage (swath width) and regular repeat cycle as MODIS. Furthermore, many have only been put into orbit quite recently. No data archives at regular time intervals exist for the past years and data are not permanently archived, particularly for West-Africa. As a result, MODIS data were considered appropriate for this study. Remote sensing techniques show the potential to map and monitor the number of wetlands. Using higher resolution data the number of dams, which is not precisely known, may also be observed. The current analyses were carried out on a monthly basis, both for performing cumulative surface water area and time series anomaly calculations. An increase in temporal resolution, through the use of 8-day composite or daily MODIS data for water detection is suggested to further characterize wetlands by their seasonal dynamics in greater detail [25].

Since heavy precipitation occurs almost exclusively during the rainy season, which increases in duration toward the South, cloud cover dominates during these periods. MODIS quality state flags from the 500 m data were applied for cloud masking, together with applying a NIR threshold to the 250 m bands. This could be further improved by incorporating the 500 m resolution blue band [24], [49]. Most images from between May and September were affected by cloud cover, which resulted in many invalid pixel values, particularly in July and August, and in considerably limited water detection. This finally led to the exclusion of 4 months (June to September) in the calculation of time series water-covered area anomalies. Radar images may offer a solution to the problem of cloud cover. However, at present no synthetic aperture radar (SAR) data archive is available for the past 13 years with regular recurrence. Envisat ASAR side swath mode (WSM) data archives are available at 150 m resolution in irregularly repeated time steps (from weekly to scarce coverage) and were recently used for creating a global dataset of permanent open water bodies [50]. ScanSAR data from TerraSAR-X are currently being recorded. Further analysis will indicate the usefulness of regular SAR time series for wetland monitoring, providing an outlook on the possibilities of data from Sentinel-1, launched in April 2014 by the European Space Agency (ESA), which will provide such regular observations in the C-band wavelength. Also related to clouds are cloud shadows, which commonly account for uncertainty in water classification [24], [49]. This was not found to have a major impact in the current work since the images are already composites based on a per-pixel quality ranking over 8 days of daily acquisitions. However, topographic shadows appeared repeatedly in the same location and were needed to be masked out using their repeated occurrence and verification with Landsat imagery, if they were not already excluded by the slope threshold based on the DEM. Burn scars resulting from controlled savannah fires as well as bushfires also tend to be subject to misclassification as water. Due to fast vegetation succession, burn scars are typically only exposed for a few weeks before grass begins to grow again. Therefore, they were excluded by their occurrence in not more than one monthly composite, apart from a region in the north-west of the study area, in Mali, where burn scars persist over large areas for about 2–3 months, resulting in misclassification. There is a lack of official reference to drought periods, on the national as well as local scales. In this work, local expert interviews served as reference to drought to compliment data available at much larger scales (i.e., the Sahel). Drought can have a very local effect due to rainfall patterns, watershed characteristics, and soil properties. Such local data would be important in order to better define and record drought on a local scale.

Based on the present results, a number of important avenues for future research are identified. It is suggested that further scientific work cover a larger spatial analysis, considering all wetlands in the area using methods developed for the case study regions in this paper. The availability of *in situ* data, and the quantification of differences related to the latitudinal gradient, natural and artificial water bodies, size classes, adjacent land use activities and vicinities to villages, as well as

further analysis of seasonal characteristics would provide great insight. Likewise, the comparative use of higher temporal and spatial resolution data is recommended.

VI. Conclusion

This work presents the application of NIR-based water monitoring using a latitudinal gradient approach applied to MODIS time series data from 2000 to 2012 for wetlands and reservoirs of semiarid Burkina Faso. The method performed well in southern and central areas but was limited by aquatic vegetation cover occurring particularly in northern natural wetlands, and cloud cover increasing toward the south. 219 wetlands larger than $0.1\ \mathrm{km}^2$, among them 68 larger than $1\ \mathrm{km}^2$, were detected in the $150\ \mathrm{km} \times 500\ \mathrm{km}$ large study area, spanning a gradient of different rainfall and land use characteristics. Five case studies consisting of two natural and three artificial wetlands are analyzed in further detail. Annual cumulative spatiotemporal observations of surface area were derived, revealing reduced water extent and duration of water coverage in the drought seasons of 2000–2001, 2004–2005, and 2011–2012. Only a few small wetlands were found to have completely disappeared during the study period, but 21 newly appearing water bodies greater than $0.5\ \mathrm{km}^2$ size were detected, among them three large water bodies.

Time series of water-covered surface area and their monthly anomalies were retrieved, and display a distinct seasonal cycle. Low surface water area peak levels and negative surface water anomalies were found to be associated with the three drought periods mentioned above, for all case study sites. The 2003–2004 and 2005–2006 seasons show the largest positive anomalies of all case study wetlands. Furthermore, the timing of dam constructions can be deduced from MODIS time series data, as shown through the example of the Yakouta reservoir, built in 2004. The successful application of remote sensing time series as a tool to monitor wetlands in semiarid areas over large areal extents and with appropriate temporal resolution is shown. Information regarding spatiotemporal dynamics is derived and related to the occurrence of drought years, indicating the potential to serve as an important drought indicator.

Acknowledgment

The authors appreciate that MODIS, SRTM, and Landsat data are provided free of charge by NOAA/USGS. They would like to thank Dr. R. Ouedraogo for valuable local advice and assistance in preparation for field work, B. M. Somandé for assistance and translation during field work, F. Betorz Martinez for assistance during field work, and J. Schaal for Landsat data preparation and extraction of water masks for validation, and also thank the reviewers for their helpful comments to improve this paper.

References

[1] UNEP, *Africa Water Atlas*. Nairobi, Kenya: Division of Early Warning and Assessment (DEWA), United Nations Environment Programme (UNEP), 2010.

[2] UNEP & ICRAF, *Climate Change and Variability in the Sahel Region: Impacts and Adaptation Strategies in the Agricultural Sector*. Nairobi, Kenya: United Nations Environment Programme (UNEP) and Headquarters of the World Agroforestry Centre (ICRAF), 2006.

[3] Food and Agriculture Organization of the United Nations (FAO), *The Sahel Crisis* [Online]. Available: http://www.fao.org/crisis/sahel/en/, accessed Jul. 2014.

[4] Famine Early Warning System Network (FEWS NET). *Food Security Outlook Updates for West-Africa* [Online]. Available: http://www.fews.net/west-africa, accessed Jul. 2014.

[5] Reliefweb, *Sahel: Food Insecurity 2011–2014* [Online]. Available: http://reliefweb.int/disaster/ot-2011-000205-ner, accessed Jul. 2014.

[6] M. Falkenmark, "The massive water scarcity threatening Africa—Why isn't it being addressed," *Ambio*, vol. 18, no. 2, pp. 112–118, 1989.

[7] R. Ouedraogo, "Fish and fisheries prospective in arid inland waters of Burkina Faso, West Africa," Ph.D. dissertation, Univ. Nat. Resour. Life Sci. (BOKU), Vienna, Austria, 2010.

[8] UNOCHA. (2010, Mar. 22). *Burkina Faso: Dwindling Rains Spur Dam Construction*. *IRIN Online News Service*. UN Office for the Coordination of Humanitarian Affairs [Online]. Available: http://www.irinnews.org/Report.aspx?ReportId=88519, accessed Jul. 2014.

[9] J. G. Lyon, *Wetland Landscape Characterization: Techniques and Applications for GIS, Mapping, Remote Sensing, and Image Analysis*. Chelsea, MI, USA: Sleeping Bear Press, 2001.

[10] S. L. Ozesmi and M. E. Bauer, "Satellite remote sensing of wetlands," *Wetlands Ecol. Manage.*, vol. 10, no. 5, pp. 381–402, 2002.

[11] T. Landmann, M. Schramm, R. Colditz, A. Dietz, and S. Dech, "Wide area wetland mapping in semi-arid Africa using 250-meter MODIS metrics and topographic variables," *Remote Sens.*, vol. 2, no. 7, pp. 1751–1766, 2010.

[12] I. Klein *et al.*, "Evaluation of seasonal water body extents in Central Asia over the past 27 years derived from medium-resolution remote sensing data," *Int. J. Appl. Earth Observ.*, vol. 26, pp. 335–349, 2014.

[13] R. S. Lunetta, J. F. Knight, J. Ediriwickrema, J. G. Lyon, and L. D. Worthy, "Landcover change detection using multi-temporal MODIS NDVI data," *Remote Sens. Environ.*, vol. 105, no. 2, pp. 142–154, 2006.

[14] T. Landmann, M. Schramm, C. Huettich, and S. Dech, "MODIS-based change vector analysis for assessing wetland dynamics in Southern Africa," *Remote Sens. Lett.*, vol. 4, no. 2, pp. 104–113, 2013.

[15] H. Xu, "Modification of normalized difference water index (NDWI) to enhance open water features in remotely sensed imagery," *Int. J. Remote Sens.*, vol. 27, no. 14, pp. 3025–3033, 2006.

[16] P. Ceccato, N. Gobron, S. Flasse, B. Pinty, and S. Tarantola, "Designing a spectral index to estimate vegetation water content from remote sensing data: Part 1 theoretical approach," *Remote Sens. Environ.*, vol. 82, no. 2, pp. 188–197, 2002.

[17] B. Gouweleeuw *et al.*, "An experimental satellite-based flood monitoring system for southern Queensland, Australia," presented at the IRSE 2011 Symp., Sydney, Australia, Apr. 10–15, 2011.

[18] C. Hu, "A novel ocean color index to detect floating algae in the global oceans," *Remote Sens. Environ.*, vol. 113, no. 10, pp. 2118–2129, 2009.

[19] L. Feng *et al.*, "Assessment of inundation changes of Poyang Lake using MODIS observations between 2000 and 2010," *Remote Sens. Environ.*, vol. 121, pp. 80–92, 2012.

[20] A. R. Huete *et al.*, "Overview of the radiometric and biophysical performance of the MODIS vegetation indices," *Remote Sens. Environ.*, vol. 83, no. 1, pp. 195–213, 2002.

[21] T. Sakamoto *et al.*, "Detecting temporal changes in the extent of annual flooding within the Cambodia and the Vietnamese Mekong Delta from MODIS time-series imagery," *Remote Sens. Environ.*, vol. 109, no. 3, pp. 295–313, 2007.

[22] Y. E. Yan, Z. T. Ouyang, H. Q. Guo, S. S. Jin, and B. Zhao, "Detecting the spatiotemporal changes of tidal flood in the estuarine wetland by using MODIS time series data," *J. Hydrol.*, vol. 384, no. 1, pp. 156–163, 2010.

[23] A. S. Islam, S. K. Bala, and M. A. Haque, "Flood inundation map of Bangladesh using MODIS time-series images," *J. Flood Risk Manage.*, vol. 3, no. 3, pp. 210–222, 2010.

[24] S. Martinis, A. Twele, C. Strobl, J. Kersten, and E. Stein, "A multi-scale flood monitoring system based on fully automatic MODIS and TerraSAR-X processing chains," *Remote Sens.*, vol. 5, no. 11, pp. 5598–5619, 2013.

[25] Y. Chen, C. Huang, C. Ticehurst, L. Merrin, and P. Thew, "An evaluation of MODIS daily and 8-day composite products for floodplain and wetland inundation mapping," *Wetlands*, vol. 33, no. 5, pp. 823–835, 2013.

[26] K. Jones *et al.*, "Monitoring and assessment of wetlands using Earth Observation: The GlobWetland project," *J. Environ. Manage.*, vol. 90, no. 7, pp. 2234–2242, 2009.

[27] H. MacKay *et al*., "The role of earth observation (EO) technologies in supporting implementation of the Ramsar Convention on Wetlands," *J. Environ. Manage*., vol. 90, no. 7, pp. 2234–2242, 2009.
[28] A. Walli *et al*., "TIGER-NET—Enabling an earth observation capacity for integrated water resource management in Africa," presented at the ESA Living Planet Symp., Edinburgh, U.K., Sep. 11–13, 2013.
[29] E. M. Haas, "Temporary water bodies as ecological indicators in West African drylands," Ph.D. dissertation, Univ. Catholique de Louvain, Louvain, Belgium, 2010.
[30] E. M. Haas, E. Bartholomé, E. F. Lambin, and V. Vanacker, "Remotely sensed surface water extent as an indicator of short-term changes in ecohydrological processes in sub-Saharan Western Africa," *Remote Sens. Environ*., vol. 115, no. 12, pp. 3436–3445, 2011.
[31] J. Gardelle, P. Hiernaux, L. Kergoat, and M. Grippa, "Less rain, more water in ponds: A remote sensing study of the dynamics of surface waters from 1950 to present in pastoral Sahel (Gourma region, Mali)," *Hydrol. Earth Syst. Sci. Discuss*., vol. 6, no. 4, pp. 5047–5083, 2009.
[32] Food Early Warning System (FEWS NET), *Burkina Faso—Livelihood Zone Map* [Online]. Available: http://www.fews.net/docs/Publications/BF_Livelihoods.pdf, accessed Jul. 2014.
[33] UNDP, *Human Development Report 2013—The Rise of the South: Human Progress in a Diverse World*. New York, NY, USA: United Nations Development Programme (UNDP), Sep. 2013.
[34] *Deutsche Gesellschaft für Internationale Zusammenarbeit (GIZ, German Development Cooperation)* [Online]. Available: http://www.giz.de/de/weltweit/329.html, accessed Jul. 2014.
[35] *RAMSAR Convention on Wetlands of International Importance* [Online]. Avalibale: http://www.ramsar.org/, accessed Jul. 2014.
[36] UNEP, *Africa: Atlas of Our Changing Environment*. Nairobi, Kenya: Division of Early Warning and Assessment (DEWA), United Nations Environment Programme (UNEP), 2008.
[37] F. Gorse, and P. Chouteau, *Projet d'assainissement collectif de la ville de Ouagadougou Office national d'eau et d'assainissement—ONEA—Agence Francaise de Developpement (French Development Agency)*, Paris, France, Jul. 2008.
[38] G. Mahe, J. E. Paturel, E. Servat, D. Conway, and A. Dezetter, "The impact of land use change on soil water holding capacity and river flow modelling in the Nakambe River, Burkina-Faso," *J. Hydrol*., vol. 300, no. 1, pp. 33–43, 2005.
[39] E. F. Vermote, S. Y. Kotchenova, and J. P. Ray (2011, Feb.), *MODIS Surface Reflectance User's Guide, Version 1.3*, MODIS Land Surface Reflectance Science Computing Facility [Online]. Available: http://modis-sr.ltdri.org/products/MOD09_UserGuide_v1_3.pdf, accessed Jul. 2014.
[40] C. L. Parkinson and R. Greenstone, *EOS Data Products Handbook*, vol. 2. Greenbelt, MD, USA: NASA Goddard Space Flight Center, Oct. 2000.
[41] J. E. Hilland *et al*., "Future NASA spaceborne SAR missions," *IEEE Aerosp. Electron. Syst. Mag*., vol. 13, no. 11, pp. 9–16, Nov. 1998.
[42] J. J. Van Zyl, "The shuttle radar topography mission (SRTM): A breakthrough in remote sensing of topography," *Acta Astronaut*., vol. 48, no. 5–12, pp. 559–565, 2001.
[43] P. Jönsson and L. Eklundh, "TIMESAT—A program for analyzing time-series of satellite sensor data," *Comput. Geosci*., vol. 30, no. 8, pp. 833–845, 2004.
[44] T. Udelhoven, "TimeStats: A software tool for the retrieval of temporal patterns from global satellite archives," *IEEE JSTARS*, vol. 4, no. 2, pp. 310–317, Jun. 2011.
[45] EM-DAT. (2009). *The International Disaster Database, CRED* [Online]. Available: http://www.emdat.be, accessed Jul. 2014.
[46] Societe Nationale d'Electricite du Burkina (SONABEL), *Data about Water Levels and Volumes*, Ouagadougou, Burkina Faso, 2013.
[47] R. M. Yang, A. Ru, H. L. Wang, Z. X. Chen, and J. Quaye-ballard, "Monitoring wetland changes on the source of the three rivers from 1990 to 2009, Qinghai, China," *IEEE JSTARS*, vol. 6, no. 4, pp. 1817–1824, Aug. 2013.
[48] M. Halabisky, L. M. Moskal, and S. A. Hall, "Object-based classification of semi-arid wetlands," *J. Appl. Remote Sens*., vol. 5, no. 1, pp. 053511-1–13, 2011.
[49] Y. Luo, A. P. Trishchenko, and K. V. Khlopenkov, "Developing clear-sky, cloud and cloud shadow mask for producing clear-sky composites at 250-meter spatial resolution for the seven MODIS land bands over Canada and North America," *Remote Sens. Environ*., vol. 112, no. 12, pp. 4167–4185, 2008.
[50] M. Santoro *et al*., "Introducing a global dataset of open permanent water bodies," presented at the ESA Living Planet Symp., Edinburgh, U.K., Sep. 09–13, 2013.

Linda Moser received the M.Sc. degree in environmental system sciences from the University of Graz, Graz, Austria, in 2008. Currently, she is pursuing the Ph.D. degree at the Department of Earth Observation, Friedrich-Schiller University Jena, Jena, Germany.

She worked as a Tutor in Remote Sensing with the University of Graz. From 2008 to 2010, she worked in earth observation science and education with the European Space Agency (ESA), in Rome, Italy. Since December 2010, she has been with the German Remote Sensing Data Center of the German Aerospace Centre (DLR), Oberpfaffenhofen, Germany. She worked in the Center for Satellite-Based Crisis Information (ZKI) performing rapid mapping from satellite data for emergency response after natural disasters and for humanitarian relief. Since October 2011, she has been a Marie Curie Early Stage Researcher within the "Copernicus Initial Operations—Network for Earth Observation Research Training" (GIONET) project, working on time-series analysis of satellite data in West-Africa with focus on wetlands to characterize environmental and human impacts related to water scarcity.

Stefan Voigt received the degree in physical geography, with special emphasis on remote sensing and physics, from Ludwig Maximilian University of Munich, Munich, Germany, in 1997. From 1997 to 2000, he was a Research Assistant with the Bern University, Bern, Switzerland, working on near real-time snow cover remote sensing for hydrological applications (Ph.D. in 2000).

Since 2000, he has been a Research Team Leader/Senior Researcher with the Earth Observation Center of the German Aerospace Center (DLR), Oberpfaffenhofen, Germany. He was coordinator of a large geo-scientific Sino-German research initiative on uncontrolled coal seam fires (2000–2008). He is an Initiator and First Coordinator of the DLR Center for Satellite-Based Crisis Information (DLR/ZKI). He has contributed and coordinated many national, European, and international research projects on the usage of Earth Observation data for crisis/disaster management, humanitarian relief, and civil security matters.

Elisabeth Schoepfer received the degree in geography from the University of Salzburg, Salzburg, Austria, in 2001, and the Ph.D. degree in geography, with special emphasis on remote sensing and geographic information science, in 2005.

After several years of experience in remote sensing working with the Center for Geoinformatics, University of Salzburg, from 2002 to 2007 and with the European Space Agency (ESA) from 2007 to 2009, she joined the German Remote Sensing Data Center (DFD), German Aerospace Center (DLR), Oberpfaffenhofen, Germany. Her research interests include humanitarian relief and human security, in which she has gained a lot of scientific and technical expertise related to crisis monitoring.

Stephanie Palmer received the B.A. degree in environmental studies and the M.Sc. degree in earth and planetary sciences from the McGill University, Montréal, QC, Canada, in 2007 and 2009, respectively. Currently, she is pursuing the Ph.D. degree in physical geography at the University of Leicester, Leicester, U.K.

After several years of research and project coordination experience, she is currently employed as an Early Stage Researcher with the Balaton Limnological Institute, Hungarian Academy of Sciences Centre for Ecological Research, Tihany, Hungary, through the Marie Curie Initial Training Network, GIONET. Her research interests include optical remote sensing of water quality constituents and on the development of novel, remote sensing-based ecological indicators through the use of time series analysis and phenology parameters.